

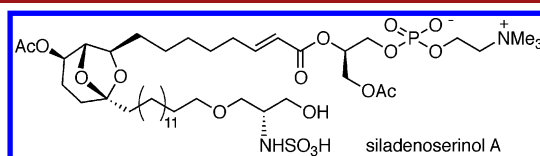
Siladenoserinols A–L: New Sulfonated Serinol Derivatives from a Tunicate as Inhibitors of p53–Hdm2 Interaction

Yuichi Nakamura,[†] Hikaru Kato,[†] Tadateru Nishikawa,[‡] Noriyuki Iwasaki,[§] Yoshiaki Suwa,[†] Henki Rotinsulu,^{||} Fije Losung,[⊥] Wilmar Maarisit,[#] Remy E. P. Mangindaan,[⊥] Hiroshi Morioka,[†] Hideyoshi Yokosawa,^{||} and Sachiko Tsukamoto^{*†}

Graduate School of Pharmaceutical Sciences, Kumamoto University, 5-1 Oe-honmachi, Kumamoto 862-0973, Japan, Bruker BioSpin K.K., 3-9 Moriya, Kanagawa-ku, Yokohama 221-0022, Japan, Bruker Daltonics K.K., 3-9 Moriya, Kanagawa-ku, Yokohama 221-0022, Japan, Faculty of Agriculture, Universitas Pembangunan Indonesia, Manado 95361, Indonesia, Faculty of Fisheries and Marine Science, Sam Ratulangi University, Manado 95115, Indonesia, Faculty of Mathematics and Natural Sciences, Christian University of Indonesia, Tomohon 95362, Indonesia, and School of Pharmacy, Aichi Gakuin University, 1-100 Kusumoto-cho, Chikusa-ku, Nagoya 464-8650, Japan
sachiko@kumamoto-u.ac.jp.

Received November 24, 2012

ABSTRACT



Siladenoserinols A–L were isolated from a tunicate as inhibitors of p53–Hdm2 interaction, a promising target for cancer chemotherapy. Their structures including the absolute configurations were elucidated to be new sulfonated serinol derivatives, each of which contains a 6,8-dioxabicyclo[3.2.1]octane unit and either glycerophosphocholine or glycerophosphoethanolamine moiety. They inhibited p53–Hdm2 interaction with IC_{50} values of 2.0–55 μ M. Among them, siladenoserinol A and B exhibited the strongest inhibition with an IC_{50} value of 2.0 μ M.

The ubiquitin–proteasome pathway consists of two systems, the ubiquitin system and the protein degradation system, i.e., the 26S proteasome. The former contains the ubiquitin-activating enzyme (E1), ubiquitin-conjugating enzyme (E2), and ubiquitin ligase (E3) and catalyzes the ubiquitination of client proteins. In addition to inhibitors targeting the proteasome, various inhibitors of the ubiquitin system have been developed. Among them, E3s recognize huge numbers of client proteins for degradation.¹ As E3 definitively determines which client proteins are ubiquitinated, a specific inhibitor against an E3

recognizing a key client protein could be a good lead for the treatment of diseases associated with degradation of the key client protein. Among many E3s, Mdm2 or Hdm2 (human Mdm2 homologue), an E3 for tumor suppressor p53,² is frequently used as a target for inhibitor development.³ The tumor suppressor p53 induces growth arrest and apoptosis upon activation by various stimuli such as DNA damage.⁴ The crystal structure of the complex composed of the 109-residue amino-terminal domain of Mdm2 and a 15-residue transactivation domain peptide of p53 revealed that Mdm2 has a deep hydrophobic cleft, to which the p53 peptide binds.⁵ Therefore, targeting Mdm2/Hdm2 is a promising way to reactivate p53, inducing apoptosis in human cancer cells.

[†] Kumamoto University.

[‡] Bruker BioSpin K.K.

[§] Bruker Daltonics K.K.

^{||} Universitas Pembangunan Indonesia.

[⊥] Sam Ratulangi University.

[#] Christian University of Indonesia.

^{*} Aichi Gakuin University.

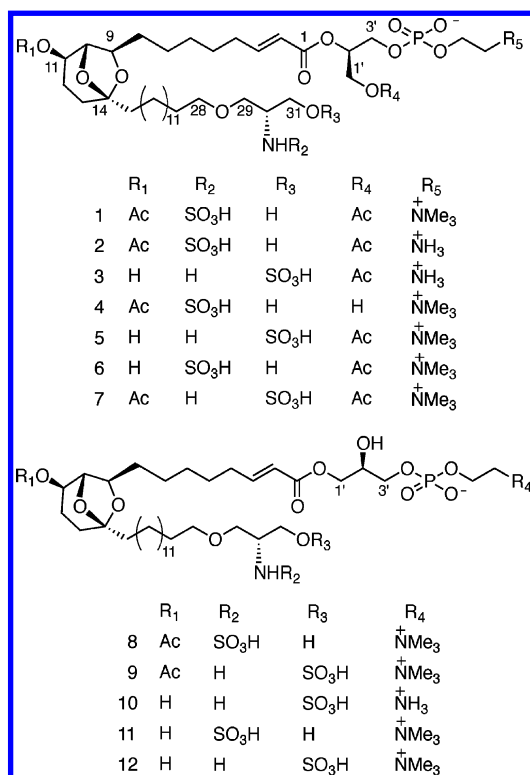
(1) (a) Pickart, C. M. *Annu. Rev. Biochem.* **2001**, *70*, 503–533. (b) Hershko, A.; Ciechanover, A. *Annu. Rev. Biochem.* **1998**, *67*, 425–479.

(2) Honda, R.; Tanaka, H.; Yasuda, H. *FEBS Lett.* **1997**, *420*, 25–27.

(3) Ashcroft, M.; Vousden, K. H. *Oncogene* **1999**, *18*, 7637–7643.

(4) Vogelstein, B.; Lane, D.; Levine, A. J. *Nature* **2000**, *408*, 307–310.

(5) Kussie, P. H.; Gorina, S.; Marechal, V.; Elenbaas, B.; Moreau, J.; Levine, A. J.; Pavletich, N. P. *Science* **1996**, *274*, 948–953.



In the course of our search for new classes of inhibitors against the ubiquitin system from natural sources, we already succeeded in isolating himeic acid A⁶ and hirtioreticulic acid A⁷ as E1 inhibitors, leucettamol A⁸ and manadosterol A⁹ as inhibitors of Ubc13 (E2)-Uev1A interaction, and (–)-hexylitaconic acid¹⁰ as an inhibitor of p53–Hdm2 interaction. In the subsequent search for more potent inhibitors of p53–Hdm2 interaction, we screened the extracts of marine invertebrates by ELISA with recombinant p53 and Hdm2 proteins¹¹ and encountered the extract of a tunicate of the family Didemnidae collected in Indonesia, which showed inhibitory activity against p53–Hdm2 interaction. Here, we report the isolation and structural determination of 12 compounds, designated siladenoseriols A–L (1–12), as inhibitors of p53–Hdm2 interaction.

A tunicate was immediately extracted with EtOH after collection. The extract was evaporated, and the aqueous residue was successively extracted with EtOAc and *n*-BuOH. The *n*-BuOH fraction, which showed inhibitory activity against p53–Hdm2 interaction, was purified by ODS column chromatography and ODS HPLC to give 1–12.

(6) Tsukamoto, S.; Hirota, H.; Imachi, M.; Fujimuro, M.; Onuki, H.; Ohta, T.; Yokosawa, H. *Bioorg. Med. Chem. Lett.* **2005**, *15*, 191–194.

(7) Yamanokuchi, R.; Imada, K.; Miyazaki, M.; Kato, H.; Watanabe, T.; Fujimuro, M.; Saeki, Y.; Yoshinaga, S.; Terasawa, H.; Iwasaki, N.; Rotinsulu, H.; Losung, F.; Mangindaan, R. E. P.; Namikoshi, M.; de Voogd, N. J.; Yokosawa, H.; Tsukamoto, S. *Bioorg. Med. Chem.* **2012**, *20*, 4437–4442.

(8) Tsukamoto, S.; Takeuchi, T.; Rotinsulu, H.; Mangindaan, R. E. P.; van Soest, R. W.; Ukai, K.; Kobayashi, H.; Namikoshi, M.; Ohta, T.; Yokosawa, H. *Bioorg. Med. Chem. Lett.* **2008**, *18*, 6319–6320.

(9) Ushiyama, S.; Umaoka, H.; Kato, H.; Suwa, Y.; Morioka, H.; Rotinsulu, H.; Losung, F.; Mangindaan, R. E. P.; de Voogd, N. J.; Yokosawa, H.; Tsukamoto, S. *J. Nat. Prod.* **2012**, *75*, 1495–1499.

(10) Tsukamoto, S.; Yoshida, T.; Hosono, H.; Ohta, T.; Yokosawa, H. *Bioorg. Med. Chem. Lett.* **2006**, *16*, 69–71.

(11) (a) González, N.; Rodríguez, J.; Jiménez, C. *J. Org. Chem.* **1999**, *64*, 5705–5707. (b) Kiyota, H.; Dixon, D. J.; Luscombe, C. K.; Hettstedt, S.; Ley, S. V. *Org. Lett.* **2002**, *4*, 3223–3226.

Siladenoserinol A (1) has the molecular formula C₄₃H₇₉N₂O₁₇PS, which was determined by HRESIMS and ¹³C NMR (Table S1, Supporting Information) spectrometries. The ¹H NMR spectrum (Table S1, Supporting Information) showed two olefin signals at δ 7.02 (dt, *J* = 15.6, 7.0 Hz) and 5.86 (d, *J* = 15.6 Hz), 18 heteroatom-bearing signals at δ 5.27 (m), 4.67 (br s), 4.27 (2H, m), 4.38 (dd, *J* = 12.0, 3.7 Hz), 4.22 (dd, *J* = 12.0, 6.5 Hz), 4.16 (br s), 4.03 (2H, t, *J* = 5.8 Hz), 3.99 (br t, *J* = 4.6 Hz), 3.65 (2H, m), 3.68 (dd, *J* = 11.0, 5.5 Hz), 3.63 (dd, *J* = 11.0, 5.3 Hz), 3.58 (dd, *J* = 9.4, 4.7 Hz), 3.51 (dd, *J* = 9.4, 6.6 Hz), 3.45 (2H, t, *J* = 6.6 Hz), and 3.43 (m), three singlet signals at δ 3.23 (9H), 2.07 (3H), and 2.03 (3H), a methylene signal at δ 2.25 (2H, br q, *J* = 7.0 Hz), and methylene/methine signals at δ 1.3–2.1. Analysis of 2D spectra, including COSY, HSQC, and HMBC spectra, showed three partial structures a–c (Figure 1). In a unit a, the COSY spectrum showed a linear connection from C-2 to C-5 and from C-8 to C-13. HMBC correlations from δ 2.25 (H-4), 1.49 (H-5), and 1.36 (H-7) to δ 30.1 (C-6) and from δ 3.99 (H-9) to δ 26.3 (C-7) secured a whole connection from C-2 to C-13. Two olefin hydrogens, H-2 and H-3, showed a coupling constant, *J*_{2,3} = 15.6 Hz, which indicated a 2*E* configuration. HMBC correlations from δ 7.02 (H-3) and 5.86 (H-2) to δ 167.3 (C-1) and from δ 2.07 (11-OCOMe) and 4.67 (H-11) to δ 172.4 (11-OCOMe) implied the presence of an α,β-unsaturated carbonyl group and an acetoxy group on

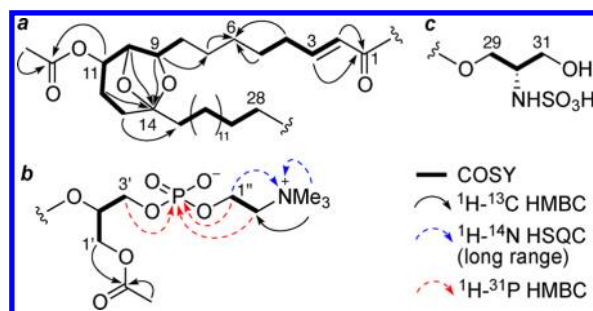


Figure 1. Partial structures a–c of 1.

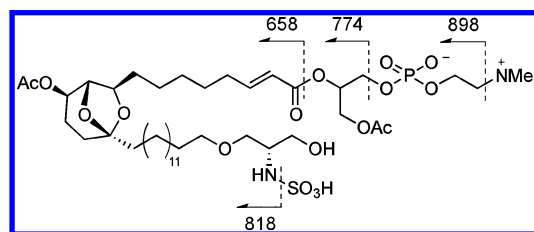


Figure 2. ESI-MS/MS analysis of 1.

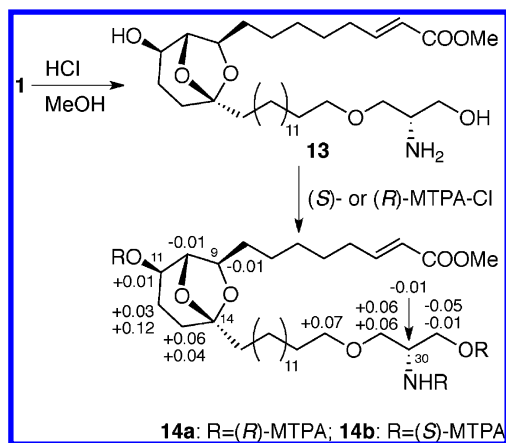
C-11, respectively. HMBC correlations from δ 3.99 (H-9), 4.16 (H-10), and 1.72 (H-12) to δ 110.5 (C-14) indicated that

(12) Mitchell, S. S.; Rhodes, D.; Bushman, F. D.; Faulkner, D. J. *Org. Lett.* **2000**, *2*, 1605–1607.

the **a** unit contained a 6,8-dioxabicyclo[3.2.1]octane skeleton (Figure 1), which is contained in known serinolipids, didemnin-serinolipids A–C¹¹ and cyclodidemniserinol trisulfate.¹² Further, the COSY spectrum and HMBC cross peaks from δ 1.52/1.74 (H₂-13) to δ 38.3 (C-15) suggested that another linear carbon chain was connected at C-14, but the COSY correlation did not define the length of the carbon chain. From these data, the **a** unit possesses the 6,8-dioxabicyclo[3.2.1]-octane core with two long carbon chains, one of which has an ester linkage. In a second unit **b**, the COSY spectrum implied the presence of 1,2,3-trisubstituted propyl [δ 4.22 (dd, J = 12.0, 6.5 Hz, H-1'), 4.38 (dd, J = 12.0, 3.7 Hz, H-1'), 5.27 (m, H-2'), and 4.03 (2H, t, J = 5.8 Hz, H₂-3')] and 1,2-disubstituted ethyl [δ 4.27 (2H, m, H₂-1'') and 3.65 (2H, m, H₂-2'')] moieties, and the ¹³C chemical shifts clearly suggested that the five carbons were bonded to hetero atoms. A singlet signal at δ 3.23 matched nine hydrogens, which defined the presence of three equivalent methyl groups. The signal (δ 3.23) had an HSQC cross peak with a carbon at δ 54.6, which indicated that the singlet signal was a methyl signal accommodated in a trimethylamino group. The HMBC spectrum showed a correlation from NMe₃ to C-2'' and a ¹H–¹⁴N HSQC (long-range) spectrum showed correlations from H₂-1'' and NMe₃ to NMe₃ (Figures 1 and S8, Supporting Information), which showed that the trimethylamino group was attached to C-2''. The presence of an acetoxy group at C-1' was revealed by HMBC cross peaks from δ 4.22/4.38 (H₂-1') and 2.03 (1'-OCOMe) to δ 172.3 (1'-OCOMe). It was noted that the carbon signals at δ 60.5 (C-1''), 64.8 (C-3'), 67.3 (C-2''), and 71.7 (C-2') appeared as doublet signals, which indicated that these carbons were coupled with a phosphorus atom. This was confirmed by detection of a ³¹P signal at δ –0.19, which showed ¹H–³¹P HMBC cross peaks with δ 3.65 (H-2''), 4.03 (H-3'), and 4.27 (H-1'') (Figures 1 and S9, Supporting Information). These data established the structure of a 2'-O-substituted glycerophosphocholine moiety. HMBC correlations from δ 5.27 (H-2') to δ 167.3 (C-1) clearly showed that the **a** and **b** units were connected through an ester linkage at C-2'. A third unit **c** was suggested to be a substituted propyl group (δ _H 3.51/3.58 (H₂-29), 3.43 (H-30), and 3.63/3.68 (H₂-31); δ _C 70.9 (C-29), 56.0 (C-30), and 63.0 (C-31)), in which heteroatoms were attached to each carbon judged by their chemical shifts. Based on the molecular formula of **1**, the **c** unit was implied to consist of C₃H₈NO₅S and the linear aliphatic chain linked to C-14 in the **a** unit was composed of the remaining residue C₁₃H₂₆, which thereby indicated that the **c** unit was a sulfonated serinol derivative (Figure 1). Siladenoserinol G (**7**) has the same molecular formula as **1**, and the NMR spectra clearly indicated that a structural difference between **1** and **7** was only the sulfonated position (δ _H 3.62/3.66 (H₂-29), 3.64 (H-30), and 4.12/4.22 (H₂-31); δ _C 68.6 (C-29), 52.3 (C-30), and 66.1 (C-31) in **7**). In order to determine the sulfonated positions in **1** and **7**, the ¹³C NMR spectra in CD₃OD and CD₃OH were measured. The differences [$\Delta\delta$ _C = δ _C(CD₃OD) – δ _C(CD₃OH)] in the ¹³C chemical shift of C-31 were –0.24 and 0.00 in **1** and **7**, respectively, which definitively showed that **1** had a hydroxy group at C-31 and a sulfamate group at C-30. In contrast, **7** had amino and sulfate groups at C-30 and C-31, respectively. The HMBC correlation from H₂-28 to C-29

(δ 70.9) in **1** clearly showed that the linear aliphatic chain attached to C-14 in the **a** unit was connected to the **c** unit through an ether linkage. In addition, ESI MS² and MS³ spectra of **1** were measured to confirm the connection among the **a**, **b**, and **c** units and their observed peaks established a planar structure, which was analyzed by NMR experiments (Figures 2 and S10, Supporting Information). The lack of coupling between H-9 and H-10 and between H-10 and H-11 revealed that the dihedral angles, H-9/H-10 and H-10/H-11, were approximately 90°. Therefore, the relative configurations were determined to be 9*R**,10*S**,11*R**,14*S**, which was supported by the NOE correlation between H-9 and H-11. In order to determine the absolute configuration, a modified Mosher's method¹³ was applied to acidic methanolysis product **13** prepared from **1** (Scheme 1). The differences in chemical shifts ($\Delta\delta$ = δ _S – δ _R) between (*R*)- and (*S*)-MTPA esters (**14a** and **14b**, respectively) clearly indicated 9*R*,10*S*,11*R*,14*S*,30*S* for **1**. In order to determine the absolute configuration of C-2', the alkaline hydrolysis product **16** prepared from **1** was subjected to esterification to give dibenzoate **17** (Scheme 2). The CD spectrum of **17** was identical to that of a dibenzoate **19** derived from a commercially available 3-*sn*-phosphatidylcholine (Figure 3). Thus, the structure of **1**,

Scheme 1. Distribution of $\delta\Delta_{S-R}$ Values for the MTPA Derivatives **14a** and **14b**



including the absolute configuration, was determined. The structure determination of other siladenoserinols **2–6** and **8–12** is described in the Supporting Information.

The inhibitory effects of siladenoserinols A–L (**1–12**) on p53–Hdm2 interaction were tested by ELISA¹⁰ (Table 1). In spite of their structural similarities, they differed in their IC₅₀ values from 2.0 to 55 μ M. Compound **1** and **2** exhibited the most significant inhibition, **8** was the next most potent inhibitor, and **7** and **12** were the weakest inhibitors. Comparing the sulfamate derivatives (R₂ = SO₃H, R₃ = H) and the corresponding sulfate derivatives (R₂ = H, R₃ = SO₃H), the sulfamate derivatives were more potent than the sulfate derivatives (IC₅₀ values: 2.0/53 μ M for **1/7**; 2.5/9.3 μ M for **8/9**;

(13) Ohtani, I.; Kusumi, T.; Kashman, Y.; Kakisawa, H. *J. Am. Chem. Soc.* **1991**, *113*, 4092–4096.

Scheme 2. Preparation of **17** and **19** from **1** and 3-*sn*-Phosphatidylcholine, Respectively

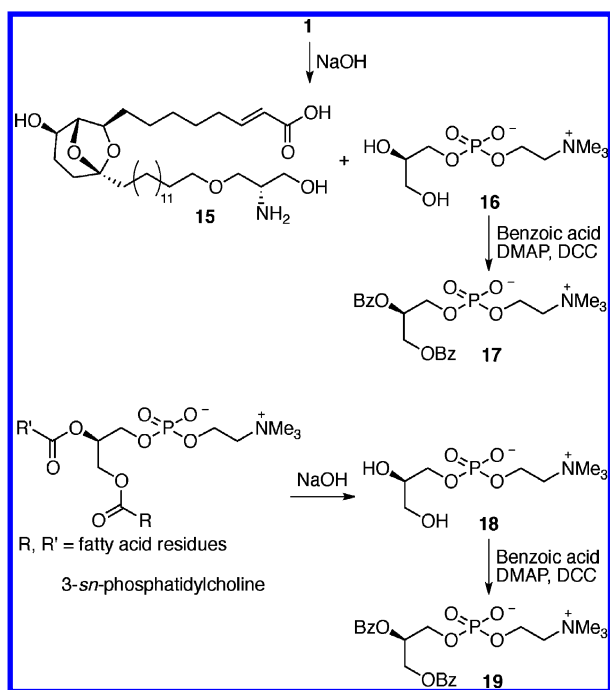


Table 1. IC₅₀ Values of **1-12** against p53-Hdm2 Interaction

compd	IC ₅₀ (μM)	compd	IC ₅₀ (μM)
1	2.0	8	2.5
2	2.0	9	9.3
3	4.0	10	11
4	7.7	11	13
5	18	12	55
6	29	nutlin-3 ^a	0.1
7	53		

^a Positive control.

group (IC₅₀ values: 2.0/7.7 μM for **1/4**). Compound **8** with an ester bond at the C-1' position of its glycerol moiety was more potent than **4** with an ester bond at the C-2' position of its glycerol moiety (IC₅₀ values: 2.5/7.7 μM for **8/4**); **1** with an ester bond at the C-2' position and an acetoxy group at the C-1' position was a little more potent than **8** with an ester bond at the C-1' position (IC₅₀ values: 2.0/2.5 μM for **1/8**). Thus, it can be inferred that the sulfamate derivatives with an ester bond at the C-2' position and acetoxy groups at the C-1' and C-11 positions exhibit the strongest inhibitory activity against p53-Hdm2 interaction.

After approval of a proteasome inhibitor, Velcade, for cancer treatment,¹⁴ inhibitors targeting the ubiquitin system including E1, E2, and E3 enzymes have also been developed, and several compounds are now undergoing preclinical and clinical trials for cancers.¹⁵ Among them, E3 inhibitors, such as Nutlin-3,¹⁶ an Mdm2 antagonist, are expected to be excellent leads for anticancer drugs, as the respective E3s recognize specific target proteins functioning in the protection against cancer progression. In this study, siladenoserinols **1-12** were found to be a new class of inhibitors against p53-Hdm2 interaction, and the first sulfonated serinolipids containing glycerophosphocholine or glycerophosphoethanolamine moieties. With respect to cytotoxic activity of **1**, it should be noted that cell viability in A549 cells was reduced to approximately 80% at a concentration of 10 μM. A study on the optimization of the inhibitory effect of siladenoserinol on the p53-Hdm2 interaction is now underway in our laboratory.

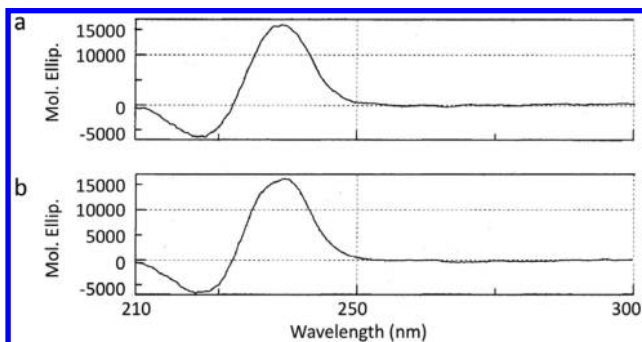


Figure 3. CD spectra of **17** (a) and **19** (b).

13/55 μM for **11/12**). In addition, in a comparison among the acetyl (R₁ = Ac) and corresponding hydroxy (R₁ = H) derivatives, the acetyl derivatives were more potent than the hydroxy derivatives (IC₅₀ values: 2.0/29 μM for **1/6**; 2.5/13 μM for **8/11**; 9.3/55 μM for **9/12**). On the other hand, a comparison between the sulfamate derivatives, **1** and **4**, led to the following result that **1**, containing the acetoxy group at a C-1' position, was more potent than **4**, lacking the corresponding acetoxy

(14) Adams, J. *Drug. Discov. Today* **2003**, *8*, 307–315.

(15) (a) Bedford, L.; Lowe, J.; Dick, L. R.; Mayer, R. J.; Brownell, J. E. *Nat. Rev. Drug Disc.* **2011**, *10*, 29–46. (b) Cohen, P.; Tcherpakov, M. *Cell* **2010**, *143*, 686–693. (c) Ande, S. R.; Chen, J.; Maddika, S. *Eur. J. Pharmacol.* **2009**, *625*, 199–205.

(16) Vassilev, L. T.; Vu, B. T.; Graves, B.; Carvajal, D.; Podlaski, F.; Filipovic, Z.; Kong, N.; Kammlott, U.; Lukacs, C.; Klein, C.; Fotouhi, N.; Liu, E. A. *Science* **2004**, *303*, 844–848.

Acknowledgment. We thank Dr. H. Kobayashi of the University of Tokyo and Prof. T. Nishikawa of Toho University for collection and identification of the tunicate, respectively. This work was supported by Grants-in-Aid for Scientific Research (Nos. 22310138 and 22406001) from the Ministry of Education, Culture, Sports, Science, and Technology of Japan and also by grants from the Astellas Foundation for Research on Metabolic Disorders and the Uehara Memorial Foundation.

Supporting Information Available. Structure determination of **2-6** and **7-12**, preparation of **14a,b**, **17**, and **19**, NMR spectral data tables, and 1D and 2D NMR spectra. This material is available free of charge via the Internet at <http://pubs.acs.org>.

The authors declare no competing financial interest.